

Design, Synthesis and Characterization of New Acenaphthoquinone derived Halogen-Substituted Oxindole Bis-Schiff Bases: In-Vitro and In-Silico Studies

Suraiya Khan¹, Malik Nasibullah^{1,*}

¹Medicinal Chemistry Laboratory-ICEIR, Department of Chemistry, Integral University, Lucknow-226026, India

*Corresponding author's email: malik@iul.ac.in, ksuraiya@iul.ac.in

ABSTRACT

In this study, a new series of halogen-substituted oxindole bis-Schiff base derivatives (5f, 5g, and 5j) were synthesized using a regioselective strategy involving temporary carbonyl protection followed by sequential condensation between halogenated isatin and acenaphthoquinone derivatives. The structural elucidation of the synthesized compounds was confirmed by FT-IR, ¹H NMR, and ¹³C NMR spectral analyses, validating the formation of the bis-imine framework. The antibacterial evaluation revealed that halogen substitution significantly influenced biological activity, with the fluorinated derivative 5g exhibiting superior inhibition against *Bacillus subtilis* and *Escherichia coli*. Molecular docking studies performed against DNA gyrase showed strong binding affinities (–5.20 to –5.60 kcal/mol) with key hydrogen bond and hydrophobic interactions involving residues Ala117, Ala118, Tyr86, and Val90, indicating stable enzyme–ligand binding. The pharmacokinetic and ADMET analysis further revealed favourable bioavailability (0.79–0.86), excellent intestinal permeability (HIA = 0.99), appropriate TPSA (70.89 Å²), and satisfactory metabolic stability (half-life ≈ 93–97 h). The combined experimental, docking, and pharmacokinetic results highlight that these halogenated oxindole bis-Schiff bases, particularly compound 5g, possess promising structural and biological characteristics for further optimization as potential antibacterial agents targeting DNA gyrase.

KEYWORDS: *bis-Schiff base; acenaphthoquinone; isatin; antibacterial activity; DNA gyrase.*

How to Cite: Suraiya Khan, Malik Nasibullah., (2025) Design, Synthesis and Characterization of New Acenaphthoquinone derived Halogen-Substituted Oxindole Bis-Schiff Bases: In-Vitro and In-Silico Studies, *Journal of Carcinogenesis*, Vol.24, No.4, 109-119.

1. INTRODUCTION

Oxindole, The increasing resistance of pathogenic bacteria to conventional antibiotics has prompted an urgent need for the development of novel antimicrobial agents with enhanced efficacy and stability to reduce health risks in human. Among various heterocyclic scaffolds, Schiff bases have garnered considerable attention due to their structural diversity, ease of synthesis, and wide range of biological activities, including antimicrobial [1], anti-cancer [2,3], antiviral, and anti-inflammatory anti-HIV [4,5], anti-malarial [6,7], and anti-bacterial [8–11] properties. Schiff bases derived from isatin, a versatile indole-based nucleus is particularly notable for their potent biological profiles.

Acenaphthoquinone, a fused polycyclic diketone, has also emerged as a valuable synthon in heterocyclic chemistry, offering rigidity and planarity to molecular frameworks, which often enhances binding interactions with biological targets. Some of the derivatives synthesized from acenaphthoquinone possess more pharmacological activities [12] like spasmolytic activity, diuretic activity, anti-coagulant activity, anti-anaphylactic activity [12–15], anti-cancer activity [16], cytotoxic activity [17,18], anti-HIV activity [19], anti-inflammatory activity [20], anti-malarial activity [21], anti-bacterial activity [22], anti-tubercular [23], anti-hyperglycemic activity [24], anti-dyslipidemic activity [25], anti-neurodegenerative activity for diseases like Alzheimer's disease, Parkinson's disease and Huntington's disease [26]. Novel *bis*-Schiff Base derivatives of isatin and acenaphthoquinone exhibits promising antibacterial activity[27].

However, the use of monoacetal-protected acenaphthoquinone in stepwise Schiff base synthesis remains underexplored.

Figure 1 shows the chemical structures of key drug leads containing either an isatin or acenaphthoquinone core, which served as the basis for designing our prototype hybrid molecules [28–32].

In this study, we report the regioselective synthesis of a novel bis-Schiff bases (**5f**, **5g** and **5j**) via condensation of a mono-Schiff base derivative of isatin with a monoacetal derivative of acenaphthoquinone, followed by thermal deprotection to unveil the second carbonyl group in situ. This strategy enables the construction of a tricyclic hybrid molecule with potentially enhanced biological properties. The synthesized compound was thoroughly characterized using FT-IR, ^1H and ^{13}C NMR spectroscopy, and its antibacterial activity was evaluated against both Gram-positive (*Bacillus subtilis*) and Gram-negative (*Escherichia coli*) bacterial strains.

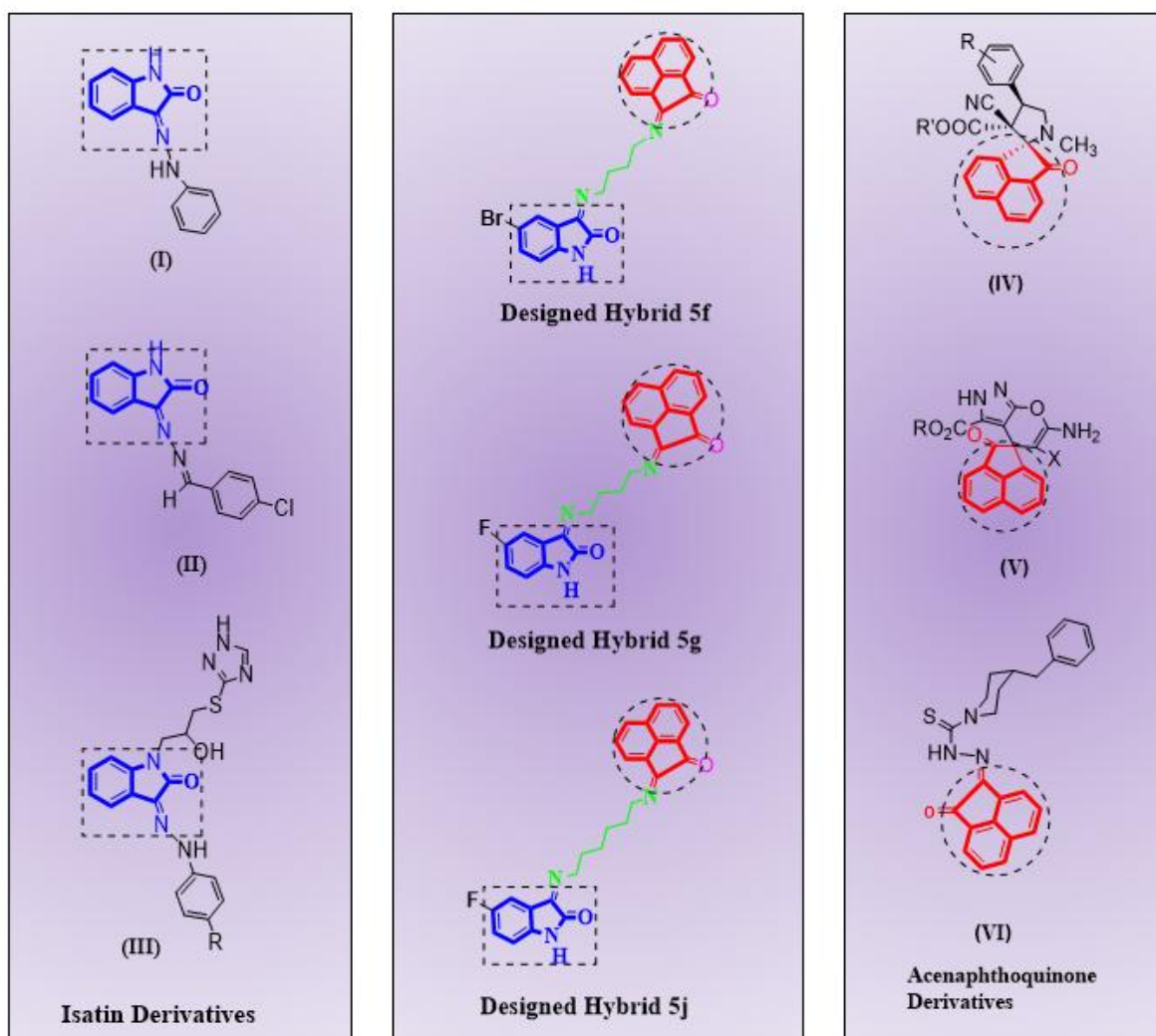


Figure.1. Schematic representation of designing Isatin–Acenaphthoquinone hybrids

2. MATERIALS AND METHODOLOGY

Materials and Instrumentation

All reagents and chemicals were procured from Sigma-Aldrich and used without further purification. Melting points were determined using a digital melting point apparatus (Gentek-934-35) and are reported uncorrected. Infrared (IR) spectra were acquired on an FT-IR spectrometer (Alpha-II 210966) over the range of $3500\text{--}500\text{ cm}^{-1}$ at the IIRC-CIF facility, Integral University, Lucknow-226026, India. NMR analyses were conducted at CSIR-Central Drug Research Institute, Lucknow-226031, India using Bruker AVANCE NEO 500 MHz high-field Fourier Transform (FT) NMR spectrometers for ^1H and ^{13}C NMR analysis using $\text{DMSO-}d_6$ as the solvent.

Synthesis of 5f, 5g and 5j

The mono-Schiff base derivatives (**3f**, **3g** and **3j**) were refluxed with (**4a**) in equimolar amounts in the presence of *p*-toluenesulfonic acid (PTSA) as catalyst for 4-6 hours to obtain (**5f'**, **5g'** and **5j'**), which further heated at 75°C to deprotect second carbonyl group of acenaphthoquinone to form bis-Schiff base derivatives (**5f**, **5g** and **5j**) as final products, further separated using standard work-up procedures and then crystallized in ethanol to obtain pure products. The purity of the

synthesized *bis*-Schiff bases was verified by thin layer chromatography (TLC) using a solvent system of diethyl ether and ethyl acetate (ratio 8:2).

(3Z)-5-bromo-3-((4-((2-oxoacenaphthylen-1(2H)-ylidene)amino)butyl)imino)indolin-2-one (5f): FT-IR (KBr, 500–3500 cm⁻¹): ν = 3183 cm⁻¹ (N–H stretching), 1738, 1720 cm⁻¹ (C=O stretching), 1656 (C=N stretching), 1603.96, 1487.57, 1465, 1439, 1420 cm⁻¹ (Aromatic C=C stretching and C–H bending), 1304.78, 1277.58, and 1212.24 cm⁻¹ (C–N stretching), 1151, 1137 cm⁻¹ (aliphatic C–N), 1059, 1015 cm⁻¹ (C–H in-plane), 894.11, 875.12, 830.22, 777.38 cm⁻¹ (C–H out-of-plane and aromatic ring deformation, C–Br). ¹H NMR (500 MHz, DMSO-d₆) δ : 10.8 ppm (s, 1H) NH, 8.5–6.8 ppm (m, 8H) ArH, 4.3 ppm (d, 2H) CH₂-N, 3.9 ppm (d, 2H) CH₂-N, 2.5–1.2 ppm (s, 3H) CH₂ chain. ¹³C NMR (100 MHz, DMSO-d₆) δ : 187.2 ppm (>C=O), 150.0–122.7 ppm (Br-Ar C), 115.6, 80.2, 60.0, 33.2, 22.1, and 14.8 ppm (Aliphatic C).

(3Z)-5-fluoro-3-((3-((2-oxoacenaphthylen-1(2H)-ylidene)amino)butyl)imino)indolin-2-one(5g): FT-IR (KBr, 500–3500 cm⁻¹): ν = 3187 cm⁻¹ (N–H stretching), 1738, 1720 cm⁻¹ (C=N, C=O stretching), 1655, 1619, 1603 cm⁻¹ (C=C aromatic), 1521 cm⁻¹, 1477, 1439, 1420 cm⁻¹ (C–H bending), 1303, 1278, 1261, 1213, 1186 cm⁻¹ (C–N stretching), 1151, 1137 cm⁻¹ (aliphatic C–N), 1059, 1015 cm⁻¹ (C–H in-plane), 954, 894, 864, 830, 808, 777 cm⁻¹ (C–H out-of-plane), 720, 686, 646, 629, 524 cm⁻¹ (aromatic ring deformation, C–F). ¹H NMR (500 MHz, DMSO-d₆) δ : 10.73 ppm (s, 1H) NH, 8.4–6.8 ppm (m, 8H) ArH, 4.7 ppm (d, 2H) CH₂-N, 4.0 ppm (d, 2H) CH₂-N, 2.6–2.1 ppm (s, 3H) CH₂ chain. ¹³C NMR (100 MHz, DMSO-d₆) δ : 187.2 ppm (>C=O), 145.1–114.5 ppm (F-Ar C), 90.2 (C–F bearing carbon), 54.0, 53.6, ppm (CH₂-N) 31.12 ppm (Aliphatic C).

(3Z)-5-fluoro-3-((6-((2-oxoacenaphthylen-1(2H)-ylidene)amino)hexyl)imino)indolin-2-one (5j): FT-IR (KBr, 500–3500 cm⁻¹): ν = 2929 cm⁻¹ (N–H stretching), 1775, 1867, 1783.87, 1737. (C=O stretching), 1643 cm⁻¹ (strong C=N stretch), 1602, 1517, 1276, and 1211.67 cm⁻¹ (Ar-C-N) 1150, 1058, 1033, 1014 (C–H in-plane), 893, 829, 777 cm⁻¹ (C–H out-of-plane), 683, 567 cm⁻¹ (aromatic ring deformation, C–F). ¹H NMR (500 MHz, DMSO-d₆) δ : 10.50 ppm (s, 1H) NH, 8.5–7.1 ppm (m, 8H) ArH, 3.7–0.8 ppm alkyl chain. ¹³C NMR (100 MHz, DMSO-d₆) δ : 187.4 ppm (>C=O), 150.1–106.5 ppm (F-Ar-C), 80 and 32 ppm (Aliphatic C).

Antibacterial activity

Method Employed (Agar Well Diffusion Technique)

The antibacterial activity of the synthesized compounds **5f**, **5g** and **5j** was assessed using the agar well diffusion method[33], a widely adopted disc diffusion technique. This method was selected due to its reliability in evaluating the inhibition potential of antimicrobial agents against pathogenic bacterial strains.

Test Microorganisms

Two bacterial strains were employed for the bioassay are Gram-positive *Bacillus subtilis* and Gram-negative: *Escherichia coli*. Both strains were obtained from a certified microbiological culture collection and maintained on nutrient agar (NA) slants at 4°C prior to use.

Preparation of Bacterial Inoculum

Bacterial cultures were grown in nutrient broth at 37 °C for 18–24 hours. The cell density of the suspensions was adjusted to an optical density of 0.1 at 600 nm using an Eppendorf spectrophotometer (AG, Germany), corresponding to approximately 1×10^8 colony-forming units per milliliter (CFU/mL).

Agar Well Diffusion Assay

Sterile nutrient agar (NA) plates were prepared and inoculated by evenly swabbing the bacterial suspensions onto the surface using sterile cotton swabs. Wells of 5 mm diameter were punched aseptically into the agar using a sterile cork borer. Test compounds **5f**, **5g** and **5j** were dissolved in DMSO and added to the wells at three different concentrations: 50, 75, and 100 µg/mL. Each concentration was tested in triplicate for statistical accuracy. Plates were incubated at 37 ± 1 °C for 24 hours.

Controls and Interpretation

Positive control is Gentamycin (1 µg/mL) and negative control is DMSO (used as the solvent). The zones of inhibition were measured in millimeters (mm) and compared to those of the controls to determine the relative antibacterial potency of the compounds. The assay was repeated three times, and average zone diameters were calculated.

Molecular Docking

The study of protein-ligand interactions at the targeted receptor active pocket is known as molecular docking. Using the Ligand lock docking tool of Silico Xplore, developed by Silico scientia Pvt. Ltd., Bangaluru, India, the molecular docking of certain compounds, namely **5f**, **5g**, and **5j**, with the E. coli DNA Gyrase protein was carried out. Protein preparation, was done on the bases of PDB file of the E. coli DNA Gyrase protein, and the ligand was prepared on the bases of the

ligand SDF files. Then molecular docking was performed as follows:

Protein preparation

The E. Coli DNA Gyrase protein was retrieved using the 6RKS PDB ID[34] during the protein preparation step, or the user could upload a protein PDB file. Since the E. coli DNA Gyrase protein contains undesired chains, heteroatoms and water molecules, the unwanted portion of the protein was cut out, and a cleaned protein was created. Because it interacts with the JHN-bound co-crystal compound, the co-crystal ligand JHN binding site serves as an active site for DNA gyrase and retains chain C of the protein for docking.

Ligand Preparation

In order to prepare the chosen ligands, i.e 5f, 5g, and 5j for molecular docking, hydrogens and Gasteiger partial charges were added. The resulting 3D pdbqt format was then created. For preparation, it needs ligand compounds in an SDF file.

Grid generation and Docking execution

The co-crystal binding pocket JHN served as the DNA gyrase protein's active site. The grid was made using the JHN co-crystal, and a configuration file was prepared with the center x,y, and z coordinates as 158.31, 147.40, and 147.61, respectively, and the size x, y, and z as 30,36, and 38, respectively. The molecular docking of the new acenaphthoquinone derived halogen-substituted oxindole bis-Schiff bases[35] was successfully submitted and finished quickly with these grid dimensions.

3. RESULTS AND DISCUSSION

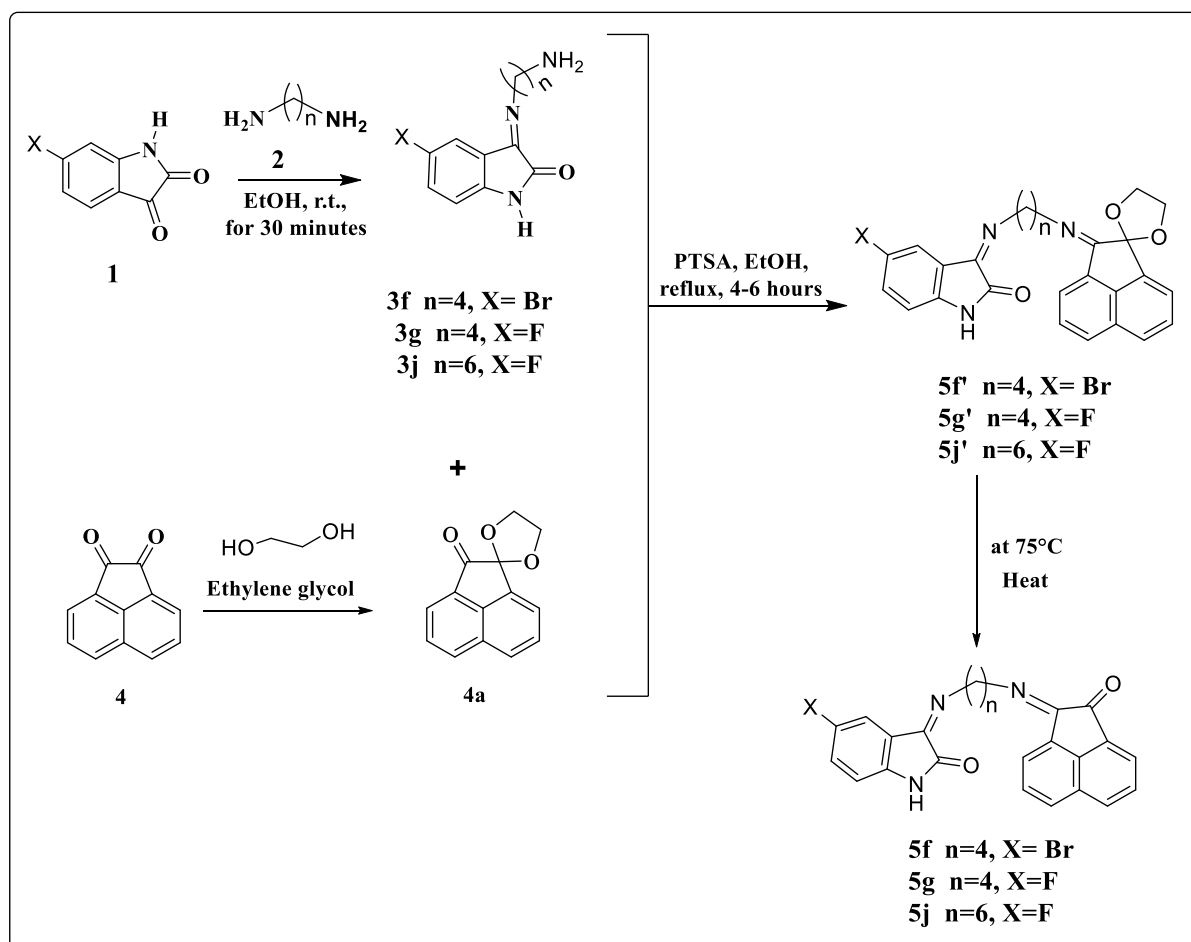
Chemistry of bis- Schiff base derivatives (5f,5g and 5j)

The key intermediates **5f**, **5g** and **5j** obtained via condensation of compounds **3f**, **3g** and **3j** with the monoacetal derivative **4a** of acenaphthoquinone, were subjected to thermal deprotection at 75 °C, resulting in the insitu hydrolysis of the acetal group. This step effectively regenerated the masked carbonyl group and allowed intramolecular nucleophilic attack by the pendant amine, yielding the tricyclic Schiff base derivatives **5f**, **5g** and **5j** with good yields and purity.

Spectral analysis of the obtained compound **5f**, confirmed its structure by molecular formula $C_{24}H_{18}BrN_3O_2$ and molecular weight 460.33 g/mol having a butyl alkyl chain ($n = 4$, $X = Br$), was synthesised by the condensation of 5-bromo isatin with diamino butane obtained as a yellow-brown solid with a melting point of 290°C and an isolated yield of 89%. The FT-IR spectrum of compound **5f** displayed characteristic absorption bands corresponding to its functional groups. A broad band at 3183.99 cm^{-1} was assigned to N–H stretching of the isatin moiety, while the absorption at 2958.41 cm^{-1} indicated aliphatic and aromatic C–H stretching vibrations. Strong carbonyl (C=O) stretching bands appeared at 1738.60 and 1720.55 cm^{-1} , attributable to the isatin and acenaphthoquinone moieties. The imine (C=N) linkage was confirmed by a prominent band at 1656.05 cm^{-1} , supporting the formation of the Schiff base. Additional bands in the range of 1603.96 , 1487.57 , 1465.74 , 1439.01 , and 1420.54 cm^{-1} were consistent with aromatic C=C stretching and C–H bending vibrations. Further absorptions at 1304.78 , 1277.58 , and 1212.24 cm^{-1} corresponded to C–N stretching, while out-of-plane aromatic C–H bending and ring deformation modes were indicated by peaks at 894.11 , 875.12 , 830.22 , and 777.38 cm^{-1} . The ^1H NMR spectrum (DMSO- d_6) exhibited a singlet at δ 10.8 ppm, attributed to the –NH proton of the isatin ring. Aromatic protons appeared between δ 8.5–6.8 ppm as doublets, triplets, and multiplets, in agreement with the substituted aromatic systems of bromo-isatin and acenaphthoquinone units. Signals at δ 4.3 and 3.9 ppm were assigned to methylene protons adjacent to nitrogen (CH₂–N), while multiplets between δ 2.5–1.2 ppm corresponded to the methylene and methyl groups of the alkyl linker. In the ^{13}C NMR spectrum, the carbonyl carbons were observed at δ 187.2 ppm, confirming the presence of ketone functionalities. Aromatic and imine carbons appeared in the range δ 150.0–122.7 ppm, and aliphatic carbons were detected at δ 115.6, 80.2, 60.0, 33.2, 22.1, and 14.8 ppm, supporting the structure of the alkyl spacer and substituted aromatic rings.

Similarly, compound **5g**, confirmed their structures by molecular formula $C_{24}H_{18}FN_3O_2$ and molecular weight 399.43. Compound **5g**, incorporating a butyl alkyl chain ($n = 4$, $X = F$), was synthesised by the condensation of 5-fluoro isatin with diamino butane, obtained as a dark yellow-brown solid with a melting point of 285 °C and an isolated yield of 86%. Its FT-IR spectrum exhibited a broad absorption at 3187, corresponding to N–H stretching of the isatin moiety. A weak band at 2360 cm^{-1} is likely due to CO₂ or overtone. Strong bands at 1738 and 1720 cm^{-1} are characteristic of C=O and C=N stretching, confirming the presence of both ketonic and imine functionalities. Aromatic C=C stretching was observed at 1655, 1619, and 1603 cm^{-1} . The presence of a nitro group is supported by the band at 1520 cm^{-1} (asymmetric N=O stretch). Peaks at 1477–1420 cm^{-1} are assigned to aromatic C–H bending, while 1303–1137 cm^{-1} indicate C–N and C–O stretching. Bands in the 1059–777 cm^{-1} region represent aromatic C–H in-plane and out-of-plane bending vibrations, and lower-frequency bands (720–524 cm^{-1}) indicate aromatic ring deformation and possible C–F stretching. The ^1H NMR spectrum revealed a broad singlet at δ 10.7 ppm, attributed to the NH proton of the isatin ring. Doublets at δ 8.4 and 8.2 ppm ($J \approx 8\text{ Hz}$) and a triplet at δ 7.8 ppm correspond to aromatic protons of the acenaphthoquinone moiety. Multiplets between δ 7.4–

7.2 ppm and a doublet at 6.8 ppm represent aromatic protons of the fluoro-substituted isatin ring. Two distinct doublets at δ 4.7 and 4.0 ppm indicate diastereotopic methylene protons adjacent to nitrogen. Additional singlets at δ 2.6, 2.5, 2.2, 2.1, and 1.2 ppm may correspond to aliphatic or linker methylene groups, or residual solvent/impurities. The ^{13}C NMR spectrum showed a peak at δ 187.2 ppm, confirming the carbonyl carbon of the isatin unit. Signals in the range δ 145.0–114.3 ppm are assigned to aromatic carbons, including those adjacent to fluorine (notably δ 115.6, 114.3, and 90.2 ppm). The downfield signal at δ 90.2 ppm suggests a C–F bonded carbon. Methylene carbons attached to nitrogen appear at δ 54.0 and 53.6 ppm, while a peak at δ 31.2 ppm corresponds to an aliphatic methylene group. The analytical data confirm the successful formation of the target Schiff base **5g** via an efficient and regioselective synthetic strategy, facilitated by temporary carbonyl protection and sequential activation steps.



Scheme 1. Proposed reaction for the synthesis of Halogen substituted di-oxindole bis-Schiff base derivatives. Under similar reaction conditions, **5j** ($n=6$, $\text{X}=\text{F}$) was synthesized by the condensation of 5-fluoro isatin with diamino hexane. It was isolated as a yellow powder with a melting point of 282°C with very good yield of 91%. The proposed molecular formula $\text{C}_{26}\text{H}_{22}\text{FN}_3\text{O}_2$ and molecular weight 427.48 was supported by spectroscopic data. The FT-IR spectrum of compound **5j** displayed characteristic absorption bands that confirmed the presence of key functional groups. Aliphatic and aromatic C–H stretching vibrations appeared at 2929.63 cm^{-1} . Multiple carbonyl (C=O) stretching bands were observed at 1975.05 , 1867.63 , 1783.87 , 1737.62 , and 1720.22 cm^{-1} , indicating the coexistence of carbonyl functionalities from the isatin and acenaphthoquinone units. The formation of the imine (C=N) bond was confirmed by a strong band at 1643.40 cm^{-1} , which is characteristic of Schiff base formation. Aromatic C=C stretching and C–H bending vibrations appeared at 1602.97 , 1517.98 , 1486.12 , 1437.93 , and 1419.42 cm^{-1} . Furthermore, C–N stretching vibrations were evident from absorptions at 1276.99 and 1211.67 cm^{-1} , while out-of-plane aromatic C–H bending and ring deformation were indicated by bands at 893.40 , 829.82 , 777.11 , 683.50 , and 567.03 cm^{-1} . In the ^1H NMR spectrum ($\text{DMSO}-d_6$), a singlet at δ 10.5 ppm corresponded to the –NH proton of the isatin moiety. Aromatic protons were detected between δ 8.5 and 7.1 ppm, appearing as multiple doublets and multiplets consistent with the substituted aromatic systems of fluorinated isatin and acenaphthoquinone derivatives. The aliphatic region showed signals at δ 3.7, 2.5, 2.3, 2.0, 1.5, 1.3, and 0.8 ppm, assigned to methylene and methyl protons within the flexible alkyl spacer connecting the two heterocyclic pharmacophores. The ^{13}C NMR spectrum revealed a carbonyl carbon at δ 187 ppm, supporting the presence of the ketone functionality. Aromatic and imine carbons appeared in the range of δ 150–109 ppm, further confirming the conjugated system. The aliphatic

carbons of the linker were observed at δ 80 and 32 ppm, corroborating the presence of the alkyl chain between the isatin and acenaphthoquinone units.

These combined spectral data substantiate the successful synthesis of compounds **5f**, **5g**, and **5j** with their proposed *bis*-Schiff base structures. The data confirm the integration of halogen substituted isatin and acenaphthoquinone pharmacophores via a flexible alkyl imine bridge, which is consistent with their anticipated antibacterial activity.

Antibacterial activities

The antimicrobial activity of the synthesized compounds (**5f**, **5g**, and **5j**) was evaluated against Gram-negative *Escherichia coli* and Gram-positive *Bacillus subtilis* using the agar well diffusion method. Gentamycin (50 μ g/mL) was used as the standard reference drug, while DMSO served as the negative control. The zone of inhibition (in mm) was measured at three different concentrations of the compounds: 50 μ g/mL, 75 μ g/mL, and 100 μ g/mL (Figure 2 & 3).



Figure 2. Antibacterial activity of *bis*-oxindole-Schiff base derivatives (5f**, **5g** and **65j**) against *Bacillus subtilis***



Figure 3. Antibacterial activity of *bis*-oxindole-Schiff base derivatives (5f**, **5g** and **65j**) against *Escherichia coli***

Against *E. coli*, compound **5g** exhibited the highest antibacterial activity with inhibition zones of 1.67 ± 0.58 mm, 3.33 ± 0.58 mm, and 4.67 ± 0.58 mm at 50, 75, and 100 μ g/mL, respectively. Compound **5f** showed moderate activity with a maximum zone of 2.67 ± 0.58 mm at 100 μ g/mL, while compound **5j** showed relatively lower activity, achieving only 1.67 ± 0.58 mm at 100 μ g/mL. The standard Gentamycin exhibited a zone of 11.67 ± 0.58 mm. For *Bacillus subtilis*, compounds generally showed better activity compared to *E. coli*, likely due to the structural differences in the bacterial cell wall between Gram-positive and Gram-negative bacteria. Compound **5g** again demonstrated superior activity with inhibition zones of 2.67 ± 0.58 mm, 3.67 ± 0.58 mm, and 4.33 ± 0.58 mm at increasing concentrations, while compounds **5f** and **5j** displayed moderate to lower activity, reaching up to 2.33 ± 0.58 mm and 4.33 ± 0.58 mm, respectively, at 100 μ g/mL. Gentamycin maintained strong inhibition with a zone of 11.67 ± 0.58 mm (Table 1).

Table 1: Antimicrobial activity of compounds against gram positive and gram negative bacteria. Values are means \pm standard deviation, n = 3

S.No.	Bacterial strain	Concentration of Compound (mm)	Gentamycin (Standard) (mm)	Control (DMSO)
-------	------------------	--------------------------------	----------------------------	----------------

		50 µg/mL	75 µg/mL	100 µg/mL	50 µg/mL	50 µg/mL
<i>E. Coli</i>						
1	5f	0.0±0.0	1.13±0.58	2.67±0.58	11.67±0.58	0.0±0.0
2	5g	1.67±0.58	3.33±0.58	4.67±0.58	11.33±0.58	0.0±0.0
3	5j	0.0±0.0	1.00±0.00	1.67±0.58	11.67±0.58	0.0±0.0
<i>B. Subtilis</i>						
4	5f	0.00±0.58	1.33±0.58	2.33±0.58	11.67±0.58	0.0±0.0
5	5g	2.67±0.58	3.67±0.58	4.33±0.58	12.33±0.58	0.0±0.0
6	5j	1.33±0.58	2.33±0.58	4.33±0.58	11.67±0.58	0.0±0.0

Results and post-docking analysis

The binding energies of particular substances with the DNA gyrase protein were retrieved and noted following the completion of molecular docking. The 3D binding interaction profiles (Fig. 4) show that the ligands are well-accommodated within the active pocket of DNA gyrase through a combination of hydrogen bonding and hydrophobic forces, which collectively contribute to complex stability. The involvement of key residues such as Ala117, Ala118, and Tyr86 in multiple complexes suggests that these amino acids play a pivotal role in ligand anchoring and inhibitory activity.

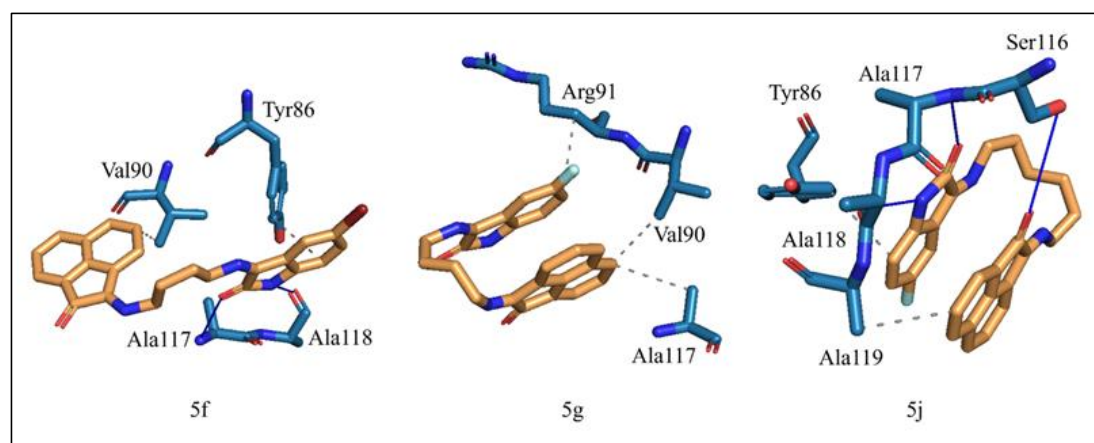


Figure 4: Binding interactions of 5f, 5g and 5j with key residues of DNA gyrase protein

The binding interactions of protein ligand complexes that were investigated using SilicoXplore's Ligand-interaction tool. Each compound exhibited mostly hydrogen bonding and hydrophobic interactions with the DNA gyrase protein, suggesting a close relationship between 5f, 5g, and 5j for DNA gyrase protein inhibition. Molecular docking studies were carried out to evaluate the binding affinity and interaction profile of the synthesized bis-Schiff base derivatives (5f, 5g, and 5j) with the *E. coli* DNA gyrase protein (PDB ID: 6RKS). The docking results, summarized in **Table 2**, reveal that all compounds exhibited significant binding affinities ranging from -5.20 to -5.60 kcal/mol, indicating a stable interaction with the enzyme's active site. Compound 5g demonstrated the highest binding affinity (-5.60 kcal/mol), forming hydrophobic interactions with Val90, Arg91, and Ala117 residues. Compound 5f displayed a comparable binding score (-5.50 kcal/mol) and established hydrogen bonds with Ala117 and Ala118, along with hydrophobic contacts involving Tyr86 and Val90. Similarly, compound 5j exhibited a binding affinity of -5.20 kcal/mol, stabilized by hydrogen bonding with Ser116, Ala117, and Ala118, as well as hydrophobic interactions with Tyr86 and Ala119.

Overall, the docking analysis suggests that the synthesized bis-Schiff base derivatives possess favourable interaction profiles with DNA gyrase, potentially leading to inhibition of bacterial replication. Among the tested compounds, **5g** exhibited the most promising binding behaviour, making it a potential lead candidate for further in silico and in vitro investigations.

Table 2: The binding interactions profile of selected compounds with DNA gyrase protein (6RKS PDB ID)

Docking Results			
Compounds	Binding Affinity (kcal/mol)	Hydrogen Bond Interacting Residues	Other Types of Interactions
5f	50	117, Ala118	86, Val90 (Hydrophobic)
5g	50		90, Arg91, Ala117 (Hydrophobic)
5j	20	116, Ala117, Ala118	86, Ala119 (Hydrophobic)

Pharmacokinetics analysis

Compounds' pharmacokinetic characteristics suggest a hit's nature based on how well or poorly they behave in the body. The PharmK-AI tool of SilicoXplore was used to retrieve the ADMET data for a subset of drugs, specifically 5f, 5g, and 5j. Molecular weight, bioavailability, human intestinal absorption, total polar surface area (TPSA), quantitative estimation of druglikeness (QED), toxicity (e.g., AMES), carcinogenicity, and skin sensitivity reaction, and excretion parameters (e.g., compound half-life and clearance) were all computed in the ADMET data results. Table 3 contains all of the pharmacokinetic information for 5f, 5g, and 5j.

Table 3: Pharmacokinetic data of selected molecules as DNA gyrase (6RKS PDB ID) protein inhibitors

Parameter	5f	5g	5j
Molecular Weight	460.33	399.42	427.47
Bioavailability	0.79	0.86	0.81
HIA (Human Intestinal Permeability)	0.99	0.99	0.99
QED	0.55	0.65	0.54
Carcinogenicity	0.37	0.33	0.38
AMES toxicity	0.49	0.69	0.58
Skin sensitivity reaction	0.72	0.62	0.61
TPSA	70.89	70.89	70.89
ClinTox	0.15	0.16	0.17
DILI	0.96	0.97	0.96
Excretion clearance	71.35	68.52	75.03
Half life	97.71	93.17	96.08

The pharmacokinetic profiles of the selected bis-Schiff base derivatives (5f, 5g, and 5j) were evaluated to predict their potential as DNA gyrase (6RKS PDB ID) protein inhibitors. The results summarized in Table 4 indicate that all compounds exhibit favourable drug-like characteristics. The molecular weights of the compounds (ranging from 399.42 to 460.33 g/mol) fall within the acceptable limit for oral drug candidates. The bioavailability scores (0.79–0.86) suggest good absorption and systemic availability, further supported by the high Human Intestinal Absorption (HIA) values (0.99 for all compounds). The quantitative estimate of drug-likeness (QED) ranged between 0.54 and 0.65, reflecting a balanced combination of physicochemical and pharmacokinetic properties.

All compounds showed moderate carcinogenicity and AMES toxicity values, indicating a low risk of mutagenicity. The skin sensitivity reaction scores were below 0.75, suggesting acceptable dermal safety. The total polar surface area (TPSA) of 70.89 Å² for each molecule indicates good permeability across biological membranes. The predicted ClinTox and DILI (Drug-Induced Liver Injury) probabilities were within safe limits, suggesting a low potential for hepatotoxicity. Moreover, the compounds exhibited moderate excretion clearance values (68.52–75.03 mL/min/kg) and satisfactory half-lives (93.17–97.71 h), implying reasonable metabolic stability. These pharmacokinetic findings indicate that the compounds 5f, 5g, and 5j possess favourable ADMET (Absorption, Distribution, Metabolism, Excretion, and Toxicity) profiles, making them promising candidates for further biological evaluation as DNA gyrase inhibitors.

4. CONCLUSION

In this study, new halogen-substituted oxindole bis-Schiff base derivatives (5f, 5g, and 5j) were successfully synthesized through a regioselective condensation strategy employing temporary carbonyl protection and sequential activation. Spectroscopic analyses (FT-IR, ¹H NMR, and ¹³C NMR) confirmed the successful formation of the targeted bis-Schiff base framework, establishing the linkage between halogen-substituted isatin and acenaphthoquinone moieties via an alkyl imine

bridge. The antibacterial screening results demonstrated that halogen substitution significantly influenced biological activity. Among the synthesized compounds, the fluorinated derivative **5g** exhibited the highest antibacterial potential against *Bacillus subtilis* and *Escherichia coli*, followed by the brominated analogue **5f**. This enhancement is attributed to the electronic and steric effects imparted by halogen atoms, which improve membrane permeability and protein–ligand interactions. Molecular docking analysis against DNA gyrase revealed favourable binding affinities for all compounds (–5.20 to –5.60 kcal/mol), with key interactions involving residues such as Ala117, Ala118, Tyr86, and Val90. The strong hydrophobic and hydrogen-bond interactions observed indicate a stable binding orientation within the active site of DNA gyrase. Furthermore, the pharmacokinetic evaluation demonstrated that all compounds possess acceptable drug-like and ADMET characteristics, including good bioavailability (0.79–0.86), high intestinal permeability (HIA = 0.99), optimal TPSA (70.89 Å²), and favourable metabolic stability (half-life ≈ 93–97 h). Low carcinogenicity, acceptable AMES toxicity, and minimal hepatotoxicity risk further support their potential as safe antimicrobial candidates. The combined experimental, docking, and pharmacokinetic results suggest that these halogenated oxindole bis-Schiff bases, particularly compound **5g**, represent promising scaffolds for the development of new antibacterial agents targeting DNA gyrase. Future studies involving molecular dynamics simulations and structure–activity relationship optimization are warranted to enhance their efficacy and pharmacological profile.

5. ACKNOWLEDGEMENT

We express our sincere gratitude to Dr. Md. Ataul Islam, Silico Scientia Private Limited, Bengaluru, India, for his valuable guidance and software support in conducting the in-silico studies and Ms. Shefali Singh, Molecular and Immunology Lab, ICEIR-3, Department of Biosciences, Integral University, Lucknow, India, for her help and assistance in-vitro studies. We are grateful to the Founder and Hon'ble Chancellor of Integral University, Lucknow, India, for providing the necessary facilities that enabled the smooth compilation of our research work. We are also thankful to the R&D dean of the Integral University for providing manuscript communication number (MCN: **IU/R&D/2025-MCN0003921**).

Funding Sources

The author(s) received no financial support for the research, authorship, and/or publication of this article.

Conflict of Interest

The author(s) do not have any conflict of interest.

Data Availability Statement

This statement does not apply to this article.

Ethics Statement

This research did not involve human participants, animal subjects, or any material that requires ethical approval.

REFERENCES

- [1] Yavari, A. Khajeh-Khezri, Recent Advances in the Synthesis of Hetero- and Carbocyclic Compounds and Complexes Based on Acenaphthylene-1,2-dione, Synthesis (Stuttg) 50 (2018) 3947–3973. <https://doi.org/10.1055/s-0037-1610209>.
- [2] J. Wang, D. Yun, J. Yao, W. Fu, F. Huang, L. Chen, T. Wei, C. Yu, H. Xu, X. Zhou, Y. Huang, J. Wu, P. Qiu, W. Li, Design, synthesis and QSAR study of novel isatin analogues inspired Michael acceptor as potential anticancer compounds, Eur J Med Chem 144 (2018) 493–503. <https://doi.org/10.1016/j.ejmech.2017.12.043>.
- [3] Q. Zhang, Y. Teng, Y. Yuan, T. Ruan, Q. Wang, X. Gao, Y. Zhou, K. Han, P. Yu, K. Lu, Synthesis and cytotoxic studies of novel 5-phenylisatin derivatives and their anti-migration and anti-angiogenic evaluation, Eur J Med Chem 156 (2018) 800–814. <https://doi.org/10.1016/j.ejmech.2018.07.032>.
- [4] W. Li, S. Zhao, F. Gao, Z. Lv, J. Tu, Z. Xu, Synthesis and In Vitro Anti-Tumor, Anti-Mycobacterial and Anti-HIV Activities of Diethylene-Glycol-Tethered Bis-Isatin Derivatives, ChemistrySelect 3 (2018) 10250–10254. <https://doi.org/10.1002/slct.201802185>.
- [5] T.L. Devale, J. Parikh, P. Miniyar, P. Sharma, B. Shrivastava, P. Murumkar, Dihydropyrimidinone-isatin hybrids as novel non-nucleoside HIV-1 reverse transcriptase inhibitors, Bioorg Chem 70 (2017) 256–266. <https://doi.org/10.1016/j.bioorg.2017.01.006>.
- [6] I. Chiyanzu, C. Clarkson, P.J. Smith, J. Lehman, J. Gut, P.J. Rosenthal, K. Chibale, Design, synthesis and anti-plasmodial evaluation in vitro of new 4-aminoquinoline isatin derivatives, Bioorg Med Chem 13 (2005) 3249–3261. <https://doi.org/10.1016/j.bmc.2005.02.037>.

- [7] R.K. Thakur, P. Joshi, P. Baranwal, G. Sharma, S.K. Shukla, R. Tripathi, R.P. Tripathi, Synthesis and antiplasmodial activity of glyco-conjugate hybrids of phenylhydrazono-indolinones and glycosylated 1,2,3-triazolyl-methyl-indoline-2,3-diones, *Eur J Med Chem* 155 (2018) 764–771. <https://doi.org/10.1016/j.ejmech.2018.06.042>.
- [8] G.-F. Zhang, X. Liu, S. Zhang, B. Pan, M.-L. Liu, Ciprofloxacin derivatives and their antibacterial activities, *Eur J Med Chem* 146 (2018) 599–612. <https://doi.org/10.1016/j.ejmech.2018.01.078>.
- [9] G.-F. Zhang, S. Zhang, B. Pan, X. Liu, L.-S. Feng, 4-Quinolone derivatives and their activities against Gram positive pathogens, *Eur J Med Chem* 143 (2018) 710–723. <https://doi.org/10.1016/j.ejmech.2017.11.082>.
- [10] D. Shukla, I. Azad, M.A. Khan, Z. Husain, A. Kamal, S.Y. Sheikh, I. Alotibi, V. Ahmad, F. Hassan, Epoxy-Functionalized Isatin Derivative: Synthesis, Computational Evaluation, and Antibacterial Analysis, *Antibiotics* 14 (2025) 595. <https://doi.org/10.3390/antibiotics14060595>.
- [11] D. Shukla, I. Azad, M.A. Khan, Z. Husain, A. Kamal, S.Y. Sheikh, I. Alotibi, V. Ahmad, F. Hassan, Epoxy-Functionalized Isatin Derivative: Synthesis, Computational Evaluation, and Antibacterial Analysis, *Antibiotics* 14 (2025) 595. <https://doi.org/10.3390/antibiotics14060595>.
- [12] L. Bonsignore, G. Loy, D. Secci, A. Calignano, Synthesis and pharmacological activity of 2-oxo-(2H) 1-benzopyran-3-carboxamide derivatives, *Eur J Med Chem* 28 (1993) 517–520. [https://doi.org/10.1016/0223-5234\(93\)90020-F](https://doi.org/10.1016/0223-5234(93)90020-F).
- [13] F.M. Abdelrazek, P. Metz, O. Kataeva, A. Jäger, S.F. El-Mahrouky, Synthesis and Molluscicidal Activity of New Chromene and Pyrano[2,3-*c*]pyrazole Derivatives, *Arch Pharm (Weinheim)* 340 (2007) 543–548. <https://doi.org/10.1002/ardp.200700157>.
- [14] F.M. Abdelrazek, P. Metz, O. Kataeva, A. Jäger, S.F. El-Mahrouky, Synthesis and Molluscicidal Activity of New Chromene and Pyrano[2,3-*c*]pyrazole Derivatives, *Arch Pharm (Weinheim)* 340 (2007) 543–548. <https://doi.org/10.1002/ardp.200700157>.
- [15] J.Y.-C. Wu, W.-F. Fong, J.-X. Zhang, C.-H. Leung, H.-L. Kwong, M.-S. Yang, D. Li, H.-Y. Cheung, Reversal of multidrug resistance in cancer cells by pyranocoumarins isolated from *Radix Peucedani*, *Eur J Pharmacol* 473 (2003) 9–17. [https://doi.org/10.1016/S0014-2999\(03\)01946-0](https://doi.org/10.1016/S0014-2999(03)01946-0).
- [16] K.S. Abou Melha, G.A. Al-Hazmi, I. Althagafi, A. Alharbi, A.A. Keshk, F. Shaaban, N. El-Metwaly, Spectral, Molecular Modeling, and Biological Activity Studies on New Schiff's Base of Acenaphthaquinone Transition Metal Complexes, *Bioinorg Chem Appl* 2021 (2021) 1–17. <https://doi.org/10.1155/2021/6674394>.
- [17] D. Chakraborty, A. Maity, C.K. Jain, A. Hazra, Y.P. Bharitkar, T. Jha, H.K. Majumder, S. Roychoudhury, N.B. Mondal, Cytotoxic potential of dispirooxindole/acenaphthoquinone andrographolide derivatives against MCF-7 cell line, *Medchemcomm* 6 (2015) 702–707. <https://doi.org/10.1039/C4MD00469H>.
- [18] T. Raj, R.K. Bhatia, A. kapur, M. Sharma, A.K. Saxena, M.P.S. Ishar, Cytotoxic activity of 3-(5-phenyl-3 H -[1,2,4]dithiazol-3-yl)chromen-4-ones and 4-oxo-4 H -chromene-3-carbothioic acid N -phenylamides, *Eur J Med Chem* 45 (2010) 790–794. <https://doi.org/10.1016/j.ejmech.2009.11.001>.
- [19] A. Hasaninejad, F. Mandegani, M. Beyrati, A. Maryamabadi, G. Mohebbi, Highly Efficient Synthesis of Spirooxindole, Spiroacenaphthylene and Bisbenzo[b]pyran Derivatives and Evaluation of Their Inhibitory Activity against Sirtuin 2, *ChemistrySelect* 2 (2017) 6784–6796. <https://doi.org/10.1002/slct.201701364>.
- [20] N. Mokarizadeh, P. Karimi, H. Kazemzadeh, N. Fathi Maroufi, S. Sadigh-Eteghad, S. Nikanfar, N. Rashtchizadeh, An evaluation on potential anti-inflammatory effects of β -lapachone, *Int Immunopharmacol* 87 (2020) 106810. <https://doi.org/10.1016/j.intimp.2020.106810>.
- [21] E. Pérez-Sacau, A. Estévez-Braun, Á.G. Ravelo, D. Gutiérrez Yapu, A. Giménez Turba, Antiplasmodial Activity of Naphthoquinones Related to Lapachol and β -Lapachone, *Chem Biodivers* 2 (2005) 264–274. <https://doi.org/10.1002/cbdv.200590009>.
- [22] Suvaiv, K. Singh, P. Kumar, S.M. Hasan, S.P. Kushwaha, A. Kumar, K.S. Ismail, S. Mujeeb, S.K. Maurya, S.M.H. Zaidi, Antibacterial Potentiality of Isatin-Containing Hybrid Derivatives: A Review, *Asian Journal of Chemistry* 35 (2023) 815–827. <https://doi.org/10.14233/ajchem.2023.27632>.
- [23] S. Mujeeb, K. Singh, M.K. Al-Zrkani, D. Al-Fahad, S.M. Hasan, M. Al Shouber, F. Ahmad, H.N. Hameed, D. Iqbal, M. Kamal, Chroman-Schiff base derivatives as potential Anti-Tubercular Agents: In silico studies, Synthesis, and Biological evaluation, *Bioorg Chem* 157 (2025) 108249. <https://doi.org/10.1016/j.bioorg.2025.108249>.
- [24] A. Kumar, R.A. Maurya, S. Sharma, P. Ahmad, A.B. Singh, G. Bhatia, A.K. Srivastava, Pyranocoumarins: A new

- class of anti-hyperglycemic and anti-dyslipidemic agents, *Bioorg Med Chem Lett* 19 (2009) 6447–6451. <https://doi.org/10.1016/j.bmcl.2009.09.031>.
- [25] F. Safari, H. Hosseini, M. Bayat, A. Ranjbar, Synthesis and evaluation of antimicrobial activity, cytotoxic and pro-apoptotic effects of novel spiro-4 H -pyran derivatives, *RSC Adv* 9 (2019) 24843–24851. <https://doi.org/10.1039/C9RA03196K>.
- S. Kumar, M. Choudhary, Synthetic Aromatic Organic Compounds Bearing 4, 4-Dimethyl-3-Thiosemicarbazide Moiety: Theoretical and Experimental Approach, *Polycycl Aromat Compd* 43 (2023) 1735–1757. <https://doi.org/10.1080/10406638.2022.2036777>.
- [26] S.S., M.N., Suraiya Khan, Novel Bis-Schiff Base Derivatives Of Isatin And Acenaphthoquinone: Synthesis, Spectral Characterization And Antibacterial Investigations, *International Journal of Environmental Sciences* 11 (2025) 2371–2379. <https://doi.org/10.64252/d8htzz71>.
- [27] P. Meshram, R. Dongre, M. Ahmed, S. Ahmed, R. Gajendhiran, A. KalilurRahiman, T. Ben Hadda, K.M. Faelelbom, A.R. Bhat, G. Tataringa, Design, synthesis and antibacterial activity of new Isatin-based Schiff base derivatives: Molecular docking, POM analysis, in silico pharmacokinetics and identification of antitumor pharmacophore sites, *J Mol Struct* 1322 (2025) 140508. <https://doi.org/10.1016/j.molstruc.2024.140508>.
- [28] F.-F. Li, W.-H. Zhao, V.K.R. Tangadanchu, J.-P. Meng, C.-H. Zhou, Discovery of novel phenylhydrazone-based oxindole-thiolazoles as potent antibacterial agents toward *Pseudomonas aeruginosa*, *Eur J Med Chem* 239 (2022) 114521. <https://doi.org/10.1016/j.ejmech.2022.114521>.
- [29] S.K. and P.S. Anshu Dandia, AN EFFICIENT SYNTHESIS AND BIOLOGICAL EVALUATION OF SPIRO[ACENAPHTHYLENE-1,2'-PYRROLIDINE] DERIVATIVES AS POTENT ANTI-INFECTIVE AGENTS, *Eur. Chem. Bull.*, 2013, 2(12), 1004-1008 (2013) 1004–1008.
- [30] C. Brita John, Y. Subba Reddy, M. Ravi Chandra, S. Selvarajan, K. Kaviyarasu, S. Kulandai Therese, Studies on the synthesis of compounds with high pharmacological activity using acenaphthoquinone, *Results Chem* 7 (2024) 101530. <https://doi.org/10.1016/j.rechem.2024.101530>.
- [31] S. Kumar, A. Hansda, A. Chandra, A. Kumar, M. Kumar, M. Sithambaresan, Md.S.H. Faizi, V. Kumar, R.P. John, Co(II), Ni(II), Cu(II) and Zn(II) complexes of acenaphthoquinone 3-(4-benzylpiperidyl)thiosemicarbazone: Synthesis, structural, electrochemical and antibacterial studies, *Polyhedron* 134 (2017) 11–21. <https://doi.org/10.1016/j.poly.2017.05.055>.
- [32] S. Singh, S. Ahmad, D. Mehta, S. Alam, Antibacterial Activity in Pyrimidine Derivatives in Lab, Using Agar Well-diffusion Method - An Update on Novel Research, *Pharmaceutical Science and Technology* 3 (2019) 40. <https://doi.org/10.11648/j.pst.20190302.12>.
- [33] A. Vanden Broeck, V. Lamour, E. coli DNA Gyrase - DNA binding and cleavage domain in State 1 without TOPRIM insertion, *Worldwide Protein Data Bank* (2019). <https://doi.org/10.2210/pdb6rks/pdb>.
- [34] walaa S.; M.N.A.; K.E.M.M.; N.E.S.; S.A.S.G. El-serwy, N Novel 5-Nitro Isatin Derivatives As DNA Gyrase Inhibitors: Synthesis, Anti-Microbial Evaluation, Molecular Docking, ADMET Predictions and QSAR Studies., *Chem Biol Lett* 7 (2020) 197–206.